









RESEARCH ARTICLE

Closing the Circulation Budget

10.1029/2024JD041738

F. Morris^{1,2} , C. M. Robinson^{3,4} , M. Reeder^{3,4} , J. Schwendike² , D. J. Parker^{2,5,6} ,
C. L. Bain⁷, and C. J. Short⁷ 

Key Points:

- The circulation budget is useful for identifying the physical processes driving weather systems even when it does not close perfectly
- An accurate representation of the subgrid scale momentum transport can very significantly improve the budget closure
- Coarsening temporal resolution beyond 30 min and spatial resolution beyond 0.15° degrades the closure in the circulation budget

Supporting Information:

Supporting Information may be found in the online version of this article.

Correspondence to:

F. Morris,
francesca.morris@ouce.ox.ac.uk

Citation:

Morris, F., Robinson, C. M., Reeder, M., Schwendike, J., Parker, D. J., Bain, C. L., & Short, C. J. (2025). Closing the circulation budget. *Journal of Geophysical Research: Atmospheres*, 130, e2024JD041738. <https://doi.org/10.1029/2024JD041738>

Received 21 JUL 2024

Accepted 2 JAN 2025

Author Contributions:

Conceptualization: F. Morris, C. M. Robinson, M. Reeder, J. Schwendike
Data curation: C. J. Short
Formal analysis: F. Morris, C. M. Robinson
Methodology: F. Morris, C. M. Robinson
Software: F. Morris, C. M. Robinson
Supervision: M. Reeder, J. Schwendike, D. J. Parker, C. L. Bain
Visualization: F. Morris, C. M. Robinson
Writing – original draft: F. Morris, C. M. Robinson

¹School of Geography and the Environment, University of Oxford, Oxford, UK, ²School of Earth and Environment, University of Leeds, Leeds, UK, ³School of Earth, Atmosphere and Environment, Monash University, Clayton, VIC, Australia, ⁴Australian Research Council Centre of Excellence for Climate Extremes, Clayton, VIC, Australia, ⁵National Centre for Climate and Atmospheric Science, University of Leeds, Leeds, UK, ⁶NORCE Norwegian Research Centre AS, Bergen, Norway, ⁷Met Office, Exeter, UK

Abstract Circulation budgets can identify physical processes underpinning tropical cyclones, mesoscale convective vortices, and other weather systems where there are interactions across scales. It is unclear, however, how well these budgets close in practice. The present study uses the rapid intensification of Tropical Cyclone Nepartak (2016) as a case study to quantify the practical limitations of calculating circulation budgets using standard reanalyses and numerical weather model data. First, we evaluate the circulation budget with ERA5. The budget residual can be reduced considerably by including contributions to circulation changes from subgrid-scale momentum transports, and reduced further with 24-hr smoothing, which dampens the discontinuous effects of data assimilation. Second, using a high-resolution Met Office Unified Model simulation, we examine how the choice of the path used (the domain boundary) affects the budget closure. Third, the truncation errors associated with numerical differentiation in time and space are investigated. The circulation budget improves as the model data are analyzed with more frequent time output intervals, and as the output grid spacing decreases. For the tropical convective examples evaluated here, the column mean budget residuals increase by up to 50% as the output intervals increase from 5 min to 3 hr. Errors also increase if the data are regridded to a coarser horizontal grid spacing and when convection straddles the domain boundary. A key result is that the circulation budget need not close for physical inferences made about the circulation and its evolution to be meaningful, thus validating the use of the technique in prior studies.

Plain Language Summary The change in atmospheric circulation can be described in terms of different processes which sum to represent the rate of change of circulation. This study investigates the reasons why the sum of the different process terms does not always equal the net circulation change exactly. One reason is that the resolutions in time and space of numerical weather model output are too low, which causes inaccuracies. Another reason is the choice of domain, and a third is the effects of processes which are not explicitly represented by the weather model. We demonstrate that it is possible to use a model output which represents the effect of nonexplicit changes to atmospheric winds to help make the different processes sum to the rate of change of circulation.

1. Introduction

The circulation Γ is the contour integral of the horizontal velocity $\mathbf{u} = (u, v)$ around a closed contour C . By Stokes' theorem the circulation is equivalent to the surface integral of the vertical component of the absolute vorticity η (which is the sum of relative vorticity ζ and planetary vorticity f) in the region S enclosed by C . Mathematically, the circulation is defined as

$$\Gamma = \oint_C \mathbf{u} \cdot d\mathbf{l} = \iint_S \eta \, dA \quad (1)$$

where $d\mathbf{l}$ denotes a derivative taken along the contour C . The circulation, therefore, encapsulates the integrated effects of smaller-scale flows within a larger-scale region, making it a powerful tool for examining scale interactions. An expression for the rate of change of the circulation, which we call the *circulation budget*, is found by integrating the vorticity equation, from which the physical processes that contribute most to changing the circulation can be isolated. Various formulations of the circulation budget have been used to analyze the dynamics

© 2025 Crown copyright and The Author (s). This article is published with the permission of the Controller of HMSO and the King's Printer for Scotland. This is an open access article under the terms of the [Creative Commons Attribution License](https://creativecommons.org/licenses/by/4.0/), which permits use, distribution and reproduction in any medium, provided the original work is properly cited.

Writing – review & editing: F. Morris, C. M. Robinson, M. Reeder, J. Schwendike, D. J. Parker, C. L. Bain

of tropical cyclones (Kutty & Gohil, 2017; Penny et al., 2016; D. J. Raymond & Carrillo, 2011; D. Raymond et al., 2014; Wang et al., 2010; Wang, 2012), mesoscale convective vortices (Cram et al., 2002; Davis & Galerneau, 2009; Fu et al., 2015), synoptic-scale waves (Schwendike & Jones, 2010; Shapiro, 1978) and jets (Morris et al., 2024), and even tornadic supercells (Noda & Niino, 2010; Roberts et al., 2020).

The circulation budget has many applications across meteorology, oceanography, and climate science. However, when used, the left and right-hand sides of the budget are often unequal; in other words, the budget does not “close.” Many of the aforementioned studies interpret budget terms regardless of how well the budget closes. It is unclear whether these discrepancies imply a deviation from the physical reality the modeled atmosphere attempts to recreate, and if so, what these deviations are. The purpose of this study is therefore to evaluate the practical limitations of calculating the circulation budget, using typical outputs from weather and climate models, and to determine whether inferences made from budgets that do not close have meaning. We now describe the formulation of the circulation budget used in this study, present a brief review of calculations of other budgets, and outline the established limitations of calculating budgets of atmospheric quantities.

1.1. Circulation Budget Formulation

The particular formulation of the circulation budget used here comes from Haynes and McIntyre (1987). The derivation assumes a shallow hydrostatic atmosphere and starts with the change in absolute vorticity on a pressure surface, which can be written in flux form as the following:

$$\frac{\partial \eta}{\partial t} = -\nabla_{xy} \cdot \mathbf{J} \quad \text{where} \quad \mathbf{J} = \begin{pmatrix} u\eta + \omega \frac{\partial v}{\partial p} - G \\ v\eta - \omega \frac{\partial u}{\partial p} + F \end{pmatrix} = u\eta - \omega \hat{\mathbf{k}} \times \frac{\partial \mathbf{u}}{\partial p} + \hat{\mathbf{k}} \times \mathbf{F}. \quad (2)$$

Here x and y denote zonal and meridional distance coordinates, respectively, $\nabla_{xy} = \left(\frac{\partial}{\partial x}, \frac{\partial}{\partial y} \right)$ is the horizontal gradient operator, $\mathbf{F} = (F, G)$ is the subgrid-scale force (often assumed to be dominated by the effects of friction), and $\hat{\mathbf{k}}$ is the unit vector normal to the pressure surface. The constituent terms physically represent the convergence of the vorticity flux ($u\eta$) and hence an accumulation of vorticity in S , the vertical tilting of horizontal vorticity into the vertical vorticity component $\left(-\omega \hat{\mathbf{k}} \times \frac{\partial \mathbf{u}}{\partial p} \right)$, and the effect of sub-gridscale forces $(\hat{\mathbf{k}} \times \mathbf{F})$.

Integrating over a closed pressure surface S enclosed by contour C gives

$$\frac{\partial \Gamma}{\partial t} = -\oint_S \nabla_{xy} \cdot \left(u\eta - \omega \hat{\mathbf{k}} \times \frac{\partial \mathbf{u}}{\partial p} + \hat{\mathbf{k}} \times \mathbf{F} \right) dS \quad (3)$$

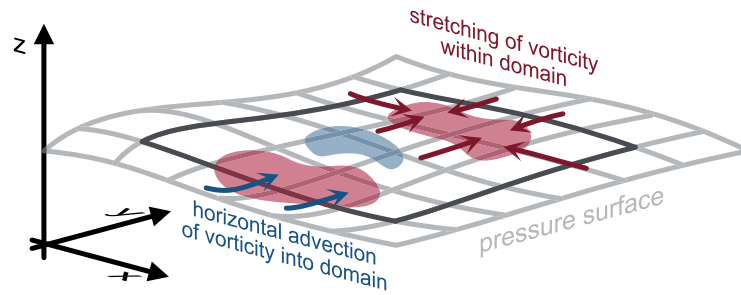
which, through the divergence theorem, can be reexpressed as the contour integral

$$\frac{\partial \Gamma}{\partial t} = -\oint_C \left(\underbrace{u\eta}_{\text{vorticity accumulation}} + \underbrace{-\omega \hat{\mathbf{k}} \times \frac{\partial \mathbf{u}}{\partial p}}_{\text{vortex tilting}} + \underbrace{\hat{\mathbf{k}} \times \mathbf{F}}_{\text{subgrid-scale forces}} \right) \cdot \hat{\mathbf{n}} dl \quad (4)$$

where $\hat{\mathbf{n}}$ represents a unit vector normal to the contour C as you move around it in infinitesimal increments of dl . Equations 3 and 4 are two equivalent expressions of the circulation budget. The terms in each version of the circulation budget characterize how different physical processes govern changes in the circulation.

Figure 1 is a schematic of the physical processes represented by the (a) vorticity accumulation and (b) vortex tilting terms. The vorticity accumulation term describes how the vertical vorticity is modulated by horizontal winds on pressure surfaces. Vorticity accumulation includes the advection of vorticity anomalies into or out of the domain, and the stretching of vorticity anomalies due to convergence in the domain. Vortex tilting relies on the

(a) vortex accumulation term



(b) vortex tilting term

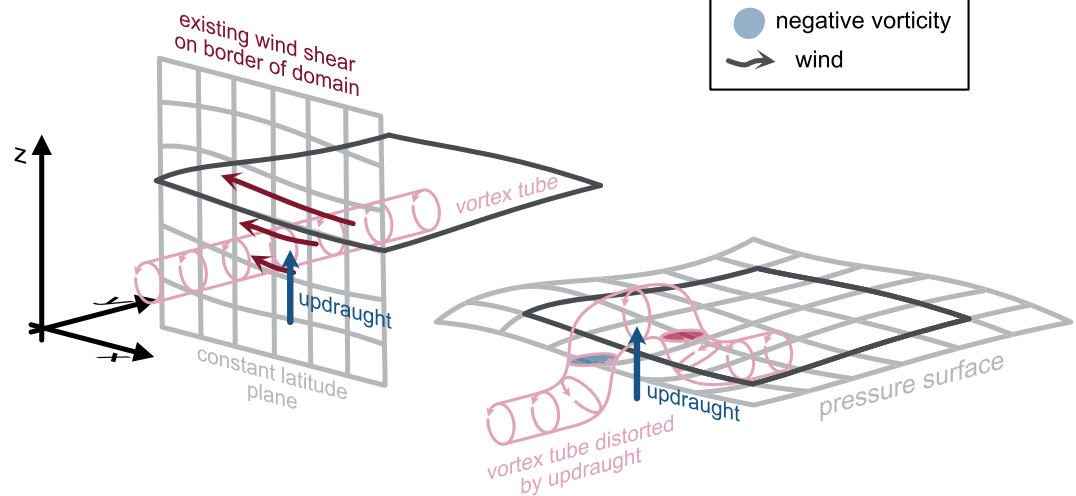


Figure 1. Schematics of the processes that change the circulation. (a) Vorticity accumulation and (b) vortex tilting. In (b), an example shear profile is illustrated by the dark red arrows; this does not necessarily reflect the shear in the Southeast Asia (the region our case study focuses on) at all times.

presence of horizontal vorticity and vertical motion. A localized vertical motion can differentially advect, or tilt, the horizontal vorticity into the vertical. This process is illustrated in Figure 1b through vortex tube lifting by an updraught on the edge of a domain. For positive $\frac{\partial u}{\partial p}$, as illustrated in the schematic, an updraught (negative ω) on the southern edge of the domain will induce a positive vertical vorticity anomaly inside the domain, which will increase the circulation (Equation 1 implies that a positive vorticity anomaly inside region S increases circulation). The positive circulation tendency induced corresponds to a positive sign overall for the tilting term when integrated anticlockwise along the southern edge with x increasing.

Analogous budgets can be formulated for any variable A that can be written in conservative form such that $\frac{\partial A}{\partial t} = \nabla \cdot \mathbf{B}$. These include budgets for thermodynamic variables such as potential temperature (Duran & Molinari, 2019), moist static energy (Kiranmayi & Maloney, 2011; Neelin & Held, 1987), or moisture, and much like circulation budget calculations, they often do not close. It should be noted that the momentum budget (Sanders & Emanuel, 1977; Stevens, 1979), while often used to evaluate processes similarly, cannot be rewritten in conservative form.

The most similar to the circulation budget is the vorticity budget (Hodur & Fein, 1977; Matthews, 2021; Shapiro, 1978; Shu et al., 2022; Stevens, 1979; Van Der Wiel et al., 2015). Many studies use the term “vorticity budget” interchangeably with “circulation budget.” Here, we define the circulation budget to be the vertical vorticity budget integrated over a pressure surface for some defined region. Equation 1 illustrates that circulation links pointwise processes within a domain (changes in vorticity anomalies) to a broader measure of the rotational part of the wind field within the region, and thus is a measure that accounts for processes over a range of spatial

scales. Therefore, circulation is useful for examining scale interactions, which are often discussed as a source of major uncertainty in tropical weather systems but are challenging to quantify. As suggested in Haynes and McIntyre (1987), it is possible even to subdivide circulation budget terms into mean and anomalous contributions which can represent processes at different scales, a technique explored in Morris et al. (2024). Furthermore, the circulation and circulation tendency are single measures of the flow in a region, whereas the vorticity and the vorticity tendency are calculated at each grid point. These quantities allow more straightforward comparisons across models, cases, and times, and smooth some of the noise that emerges in grid-cell-by-grid-cell calculations.

1.2. Budget Calculation Limitations

Often the utility of budget studies is limited due to inaccuracies in the calculation of the terms in the equation. Key errors result from the representation of the subgrid-scale forces, truncation errors associated with differentiation and integration of model outputs, and the assumptions made in the derivation of the original equation. We discuss these three issues in turn.

The subgrid-scale forces (represented by F) are generally not retained from model runs, which means they cannot be accurately calculated. These terms may be available in reanalyses such as ERA5, but they require large amounts of disk space and often are not saved in favor of saving output at higher temporal or spatial resolution. Consequently, the first aim of the current work is to assess how well the circulation budget closes without knowing F .

Truncation errors due to insufficient temporal or spatial resolution, as well as the choice of numerical methods used for differentiation and integration, may also lead to errors. Numerical techniques for solving the governing equations in models are designed for accuracy and efficiency, but are difficult to replicate in offline analysis. Chen et al. (2020) and Kanamitsu and Saha (1996) both demonstrate that significant budget errors are associated with the use of different numerical techniques in models and postprocessing. Ideally, budget terms would be computed by the model solver and saved along with other dynamical fields, so that the same numerical scheme could be used. In practice, however, many researchers are unable to run high-resolution simulations with customized outputs, and so rely on existing model outputs. Budget calculations will, therefore, often use first- and second-order finite-differencing schemes, and because models typically do not output data at every time step, they will have lower-resolution time intervals to calculate derivatives. Therefore, another aim of the current work is to evaluate the magnitude of truncation errors associated with numerical differentiation and integration, particularly at varying resolutions, and to establish the practical temporal and spatial resolutions needed to satisfactorily close the circulation budget.

The circulation budget in pressure coordinates assumes a shallow, hydrostatic atmosphere. These assumptions do not hold for a model with a nonhydrostatic dynamical core and a deep atmosphere, likely introducing errors into the budget. In particular, the assumption may not hold in convection-rich areas where the atmosphere is likely further from hydrostatic equilibrium. Here, there is reason to believe that the circulation budget may be sensitive to the contour chosen. When convection wholly within the domain tilts horizontal vortex lines into vertical lines, a vorticity dipole is formed, but its opposite contributions to circulation vanishes when averaged over the whole domain. Convection near the domain boundary could produce dipoles that lie partially in the domain (Morris et al., 2024), and whose contribution to the circulation need not vanish. Hence, a third aim of the current work is to evaluate the sensitivity of the circulation budget to the choice of the domain, which can be considered a proxy for the presence of convective activity and thus the deviation from hydrostatic equilibrium.

Taken together, the effects of subgrid-scale terms, spatiotemporal resolution, and domain choice will each affect the closure of the circulation budget. In this paper, we aim to provide an evaluation of the limitations in calculating the budget and thus, as our final aim, determine whether the conclusions drawn from inaccurate circulation budget calculations are meaningful.

2. Data, Methodology, and Case Selection

Our investigation into the circulation budget focuses on Southeast Asia (SEA) around the time at which Typhoon Nepartak (2016) rapidly intensified. The reason for this choice is the availability of a twelve-member convection-permitting ensemble simulation with the Met Office Unified Model (MetUM). The simulations have a horizontal grid spacing of 4.4 km and use the RAL1-T configuration (Bush et al., 2020). The MetUM uses the Even Newer

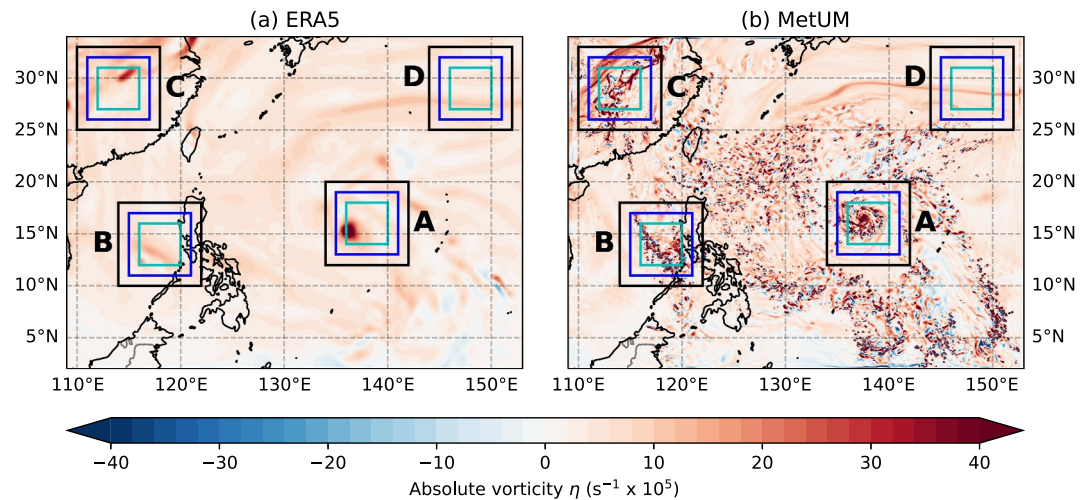


Figure 2. A snapshot of absolute vorticity (η , in 10^{-5} s^{-1}) at 700 hPa, at 01 UTC on 5 July 2016, (a) in the ERA5 reanalysis and (b) simulated by an MetUM ensemble member. Case study regions are outlined by the black ($8 \times 8^\circ$), blue ($6 \times 6^\circ$), and cyan ($4 \times 4^\circ$) boxes labeled A (Typhoon Nepartak), B (an oceanic MCS), C (an MCS over land), and D (oceanic region with least active convection).

Dynamics for General atmospheric modeling (ENDGame) nonhydrostatic dynamical core, which uses a semi-implicit semi-Lagrangian (SISL) solver (Wood et al., 2014), and its model time step is 75 s. Greater detail about the model simulations and their setup can be found in Hardy et al. (2021).

The circulation budgets based on the high-resolution MetUM simulations are compared to circulation budgets based on the ERA5 reanalysis for the same time (Hersbach et al., 2020). The reanalyses have a temporal spacing of 1 hr and a horizontal grid length of 0.25° . ERA5 is based on the European Centre for Medium-Range Weather Forecasting's (ECMWF's) Integrated Forecasting System (IFS), a spectral model with a hydrostatic dynamical core, which also uses an SISL solver. The model time step is typically 12 min.

The circulation budgets are calculated in four distinct domains, labelled A–D, and illustrated in Figure 2. The domains cover (A) part of Nepartak's track, (B) an MCS organized into a squall line over the ocean, (C) an area of organized convective activity over the land, and (D) an area over the ocean with minimal active convection. Note that Nepartak's track varies between the ERA5 reanalysis (Figure 2a) and MetUM simulations (Figure 2b); this is because the reanalysis is constrained by observations, whereas the MetUM simulation is free-running (The simulation was initialized at 12 UTC on 2 July 2016, so the time shown in Figure 2 is at T+61 hr). For each domain, we consider three boxes with sizes $8 \times 8^\circ$, $6 \times 6^\circ$, and $4 \times 4^\circ$, to test the sensitivity of the budget to the area of the domain.

The circulation and instantaneous circulation budget terms are calculated around each box for each model output interval between 13 UTC on 2 July to 07 UTC on 5 July 2016 in both the ERA5 reanalysis and the MetUM simulations. The instantaneous circulation budget terms calculated are the vorticity accumulation ($-\oint_C \mathbf{u} \eta \cdot \hat{\mathbf{n}} dl$) and vortex tilting ($\oint_C \omega \hat{\mathbf{k}} \times \frac{\partial \mathbf{u}}{\partial p} \cdot \hat{\mathbf{n}} dl$). The subgrid-scale terms are not trivial to calculate in either the ERA5 reanalysis or the MetUM simulations due to availability of data. The calculation of subgrid-scale terms is discussed in more detail toward the end of this section.

The circulation tendency is calculated using centered finite difference numerical differentiation. First, the circulation tendency is calculated from the differences between the model output time intervals. Later, the circulation tendency in the model is calculated with different values of Δt , simulating different model output time steps. Δt ranges from the highest-resolution time output of 5 min to a time interval of 6 hr. For this reason, analysis in the subsequent sections largely focuses on the time steps at 6-hr intervals from T+1 hr after the start of the model: 13 UTC on 2 July 2016.

The circulation and circulation budget terms are calculated on pressure levels. Although most ERA5 data could be downloaded on pressure levels directly, the subgrid-scale wind tendency was only output on model levels, and therefore must be interpolated onto pressure levels. The MetUM output is on hybrid height levels, and so the data are interpolated onto pressure levels. Because the vertical velocity from the MetUM was output in height coordinates, these data must be converted into pressure tendency, ω , for use in the circulation budget formulation in Equation 4. The linear numerical interpolation used may introduce errors into the calculations: in particular, the conversion between vertical velocity w and pressure tendency ω may introduce inaccuracies because the calculation assumes hydrostatic balance, which is not satisfied in the nonhydrostatic MetUM dynamical core.

The subgrid-scale force in ERA5 is stored in a field called the “mean eastward/northward wind tendency due to parameterizations.” This field includes the effects of all model parameterizations except for numerical diffusion. All interpolated values on pressure levels below the surface are set to zero. The parameterized wind tendencies are used to represent the vector \mathbf{F} , which are directly used in the budget calculation of $-\oint_C \hat{\mathbf{k}} \times \mathbf{F} \cdot \hat{\mathbf{n}} dl$.

In contrast to ERA5, the MetUM simulations store only the turbulent stress tensor's horizontal components, τ_{xz} and τ_{yz} . Following Hardy et al. (2021), the components of the subgrid-scale forces in the y and x directions, F_{xy} and F_{yx} , are related to the turbulent stress tensor according to the expressions

$$F_{xy} = \frac{1}{\rho} \frac{\partial \tau_{xz}}{\partial z}; \quad F_{yx} = \frac{1}{\rho} \frac{\partial \tau_{yz}}{\partial z}. \quad (5)$$

From Equation 5, their contribution to the circulation budget is calculated as $\hat{\mathbf{k}} \times \mathbf{F} = F_{yx} \hat{\mathbf{i}} - F_{xy} \hat{\mathbf{j}}$.

3. Closing the Circulation Budget in the ERA5 Reanalysis

We first examine the circulation budget closure in the ERA5 reanalysis. Figure 3 shows time series and vertical profiles of the circulation budget terms for the four regions (Figure 2). For the time series, the budget terms are smoothed by a 24-hr moving average to remove the diurnal cycle. In all regions, the RHS sum of the circulation budget terms is largely dominated by the accumulation term (blue line) with the tilting (orange line) and subgrid-scale (green line) terms making smaller contributions. For region (A), the RHS sum dramatically changes from positive to negative around 05 July 2016 (Figure 3a), corresponding with when Typhoon Nepartak moves through the region. At 700 hPa, the circulation budget closes reasonably well after the subgrid-scale forces are added, that is, the solid gray line (circulation tendency) closely matches the sum of RHS terms (solid black line) throughout the whole period, staying within 20% of the peak RHS values at almost all times. However, removing the subgrid term from the budget substantially worsens the closure (dashed black line), especially when the subgrid term is large as the typhoon moves through the region. The vertical profile of budget terms (Figure 3b) also shows that the budget closure is better when including the subgrid term, especially at low levels (900–1,000 hPa).

The results are largely similar for the other three regions. For region (B), which is the MCS, the budget at 700 hPa closes substantially better from 4 July after the inclusion of subgrid-scale forces. Note, however, that the closure is worse before 4 July (Figure 3c). The vertical profiles show a similar closure (Figure 3d). For region (C), which is located over land, the time series (Figure 3e) shows consistent improved budget closure, although there are still some small systematic residuals (e.g., from 2 to 4 July). However, the differences in the vertical profiles are minor (Figure 3f). Finally, region (D), located in clear conditions over the ocean, has a small friction term, and the budget closure is good regardless of whether the friction is included or not (Figures 3g and 3h). Although the inclusion of the subgrid-scale terms typically improves the closure, errors remain, which may result from the inaccurate calculation of the subgrid-scale parameterizations, or other factors such as inaccurate time derivatives or the difference in numerical differentiation techniques.

How can we objectively measure how well the budget closes? Figure 4 shows time-pressure Hovmöller plots of the circulation tendency and residual for Typhoon Nepartak (region A). The residuals are on average smaller than the circulation tendency, and they vary in both time and pressure, often changing sign. However, there are also coherent structures in the residuals, suggesting both random and systematic errors.

Panels (b) and (c) of Figure 4 show budget residuals without any temporal smoothing. There is time-varying structure in the residuals, most notably every 12 hr around 0600 and 1800 UTC, which is most likely due to the effect of the data assimilation cycle on the reanalysis. While data assimilation is designed to make the model

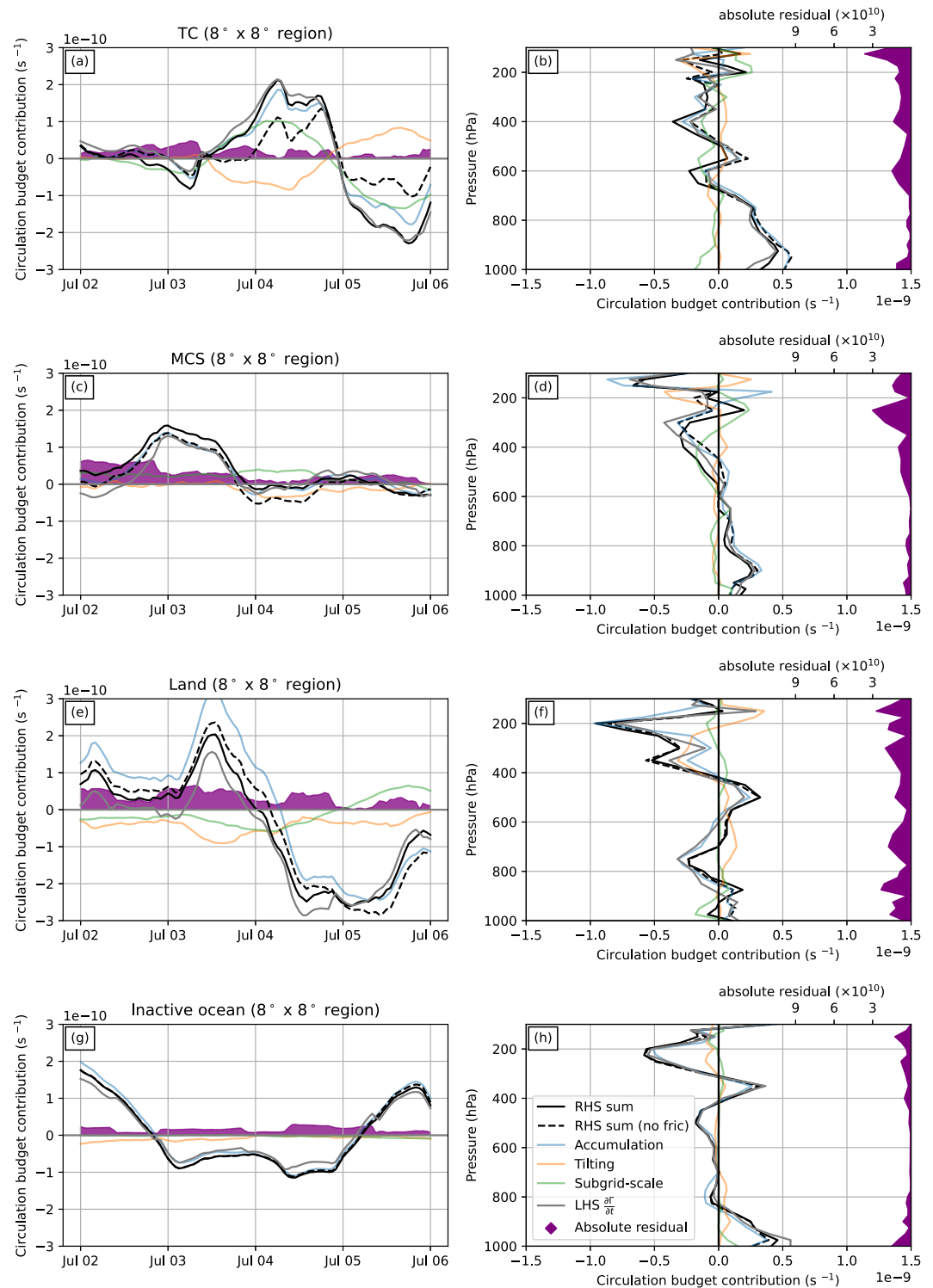


Figure 3. ERA5 circulation budget terms calculated around the four regions. Left panels show the time series of budget terms at 700 hPa, and right panels show vertical profiles of budget terms at 01 UTC on 05 July 2016. The colored lines indicate the vorticity accumulation term (blue), the tilting term (orange), and the subgrid-scale friction term (green). The black line is the sum of the three RHS terms, and the dashed black line is the sum of accumulation and tilting terms (no friction). The gray line is the circulation tendency $\frac{\partial \Gamma}{\partial t}$ at the same time around the box, calculated at the time output interval $\Delta t = 1$ hr. The purple shaded region is the absolute residual of the budget.

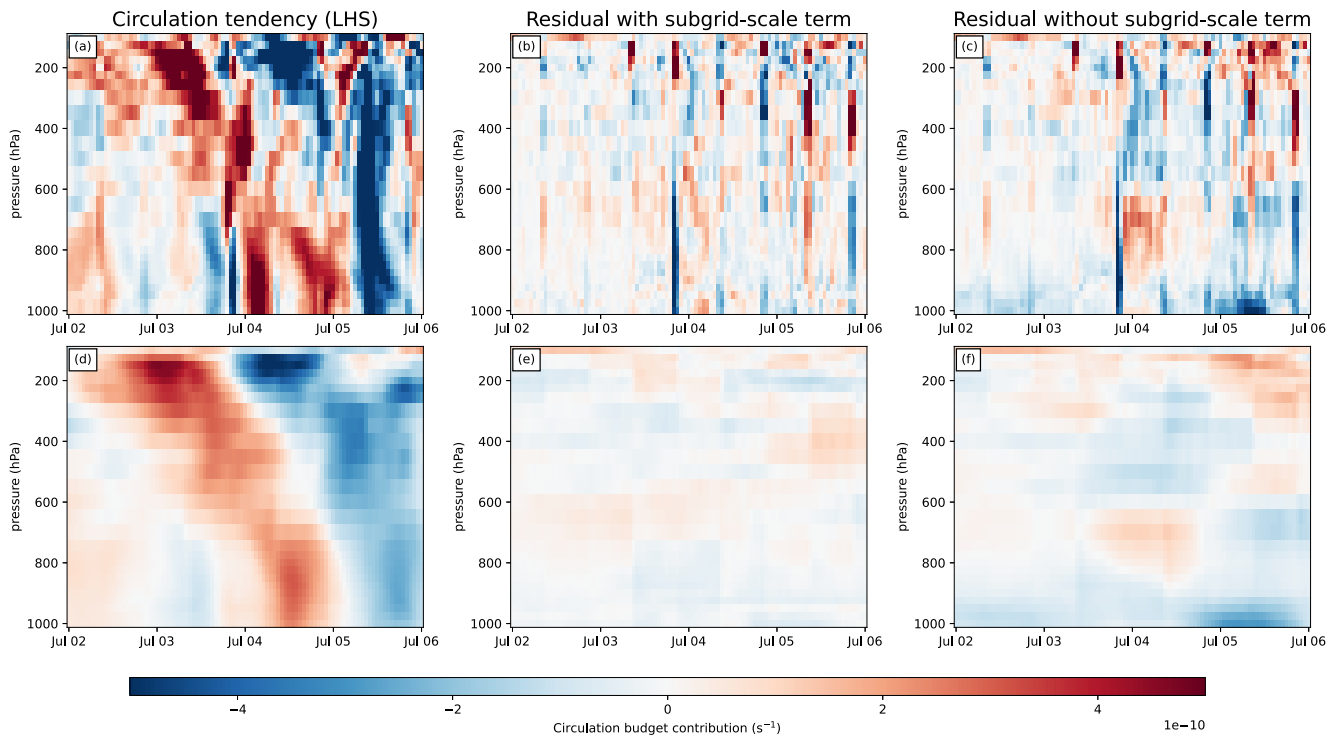


Figure 4. Time-pressure Hovmöller plots of the circulation tendency (panels a and d) and the residual term in the budget around Typhoon Nepartak (region A), including (panels b and e) and excluding (panels c and f) the subgrid-scale term. Panels (d–f) have been smoothed by a 24-hr moving average.

more realistic by applying incremental changes to bring the model closer to observed quantities in the atmosphere, it does this by modifying the results of the model which are simply the numerical solutions to the atmosphere's governing equations. As a result, the data assimilation cycle introduces unphysical changes in the budget—pushing it closer toward reality but away from solutions to the equations that describe a shallow, hydrostatic atmosphere, and thus away from perfect budget closure. Including the subgrid-scale term appears to have little effect on removing these large residuals.

Panels (e) and (f) of Figure 4 show the same residuals after applying a 24-hr moving average. In these cases, the effects of data assimilation are largely removed, resulting in smaller residuals overall. Here, the effect of including the subgrid-scale term becomes more apparent, particularly at low-to-mid levels (below 600 hPa) around 5–6 July, where a persistent negative residual is largely removed when including the subgrid term. Residuals at higher levels are also reduced, but to a lesser extent. Furthermore, the smoothed circulation tendency (panel d) shows a similar structure to its unfiltered counterpart (panel a), suggesting that the smoothed circulation budget retains the fundamental signal, as well as improves the closure.

To measure how well the budget closes overall, we integrate along the vertical profile of the mean absolute residual, and normalize by the interval of integration, described by the equation

$$\text{NCIMAD} = \frac{1}{p_{\max} - p_{\min}} \int_{p_{\max}}^{p_{\min}} \overline{|\text{LHS} - \text{RHS}|} dp \quad (6)$$

where p_{\max} and p_{\min} denote the maximum and minimum pressure levels examined, respectively, and the overbar denotes a time average. We will refer to the metric as the normalized column-integrated mean absolute difference (NCIMAD). A smaller value of NCIMAD indicates a better closure of the circulation budget. The value allows us to compare closure across different regions, time steps, combinations of terms (with or without subgrid-scale), and combinations of postprocessing (smoothing), for a fixed domain size (here, $8^\circ \times 8^\circ$).

The NCIMAD over the study period for each of the regions (A–D) is shown in Table 1. NCIMAD is smallest in all four regions when both the subgrid-scale term and smoothing are included, and largest when both are excluded.

Table 1

Normalized Column-Integrated Mean Absolute Difference Calculated for ERA5 Data During the Simulated Period Around the Regions (A–D) Shown in Figure 2

	With subgrid-scale friction. With smoothing.	With subgrid-scale friction. Without smoothing.	Without subgrid-scale friction. With smoothing	Without subgrid-scale friction. Without smoothing.
Region A	2.63	7.40	5.23	8.66
Region B	3.23	7.33	4.14	7.78
Region C	5.16	11.9	6.30	12.6
Region D	1.92	4.04	2.45	4.41

Note. All values are multiplied by 10^{-11} and have units s^{-1} . The four cases per region as are in Figure 4.

Smoothing reduces the NCIMAD by a factor of more than a half when the subgrid-scale term is also included, indicating that it improves the closure of the budget substantially. With smoothing, including the subgrid term substantially reduces the NCIMAD, most notably in region A where it is approximately halved, indicating that subgrid-scale processes such as tendencies from convective parameterization are playing a significant role in modulating the circulation, which is consistent with the convective-scale processes involved in TC propagation and maintenance. Region C has the largest NCIMAD overall, likely due to the complications of the terrestrial boundary layer.

These results suggest that the circulation budget closes very well in the reanalysis when the subgrid-scale momentum fluxes are known and available to calculate the friction term accurately. In particular, the subgrid-scale force term appears to be a vital part of the budget for strong turbulent circulations and over the land where it cannot be ignored. The effects of data assimilation on the budget can also be reduced by applying a simple smoothing algorithm. However, note that this smoothing may also remove some detail in the convective signal which may be of interest at higher temporal resolutions.

4. Closing the Circulation Budget in the MetUM

To determine the effects of changing the output time interval and spatial grid length on the closure of the circulation budget, we repeat the circulation budget calculation using the MetUM simulation with an output interval of 5 min and a grid spacing of 4.4 km. In this section, we calculate the circulation budget terms from the MetUM simulation, and examine how the closure varies as the subgrid scale contributions are or are not included, and when sampling different regions which represent different convective regimes.

As an illustration, Figure 5 shows vertical profiles of the circulation budget at the instant of the snapshot in Figure 2 for the $8 \times 8^\circ$ boxes around each of the domains (a–d) plotted in purple in Figure 2. As for the right-hand column of Figure 3, circulation budget terms are shown in the faded colored lines, with their sum shown as the black line, denoting the total of the RHS of Equation 4.

As in ERA5, the vorticity accumulation (blue line) dominates the budget, accounting for the vortex stretching and the advection of vorticity anomalies in or out of the box, while the subgrid-scale term is typically smallest in magnitude, but is noisier in the MetUM calculations than ERA5. Otherwise, the patterns are similar to the ERA5 budgets, except for a noticeable anticyclonic circulation tendency aloft in the MetUM TC region budget (Figure 5a) which does not appear in ERA5. The discrepancy is possibly due to the different cyclone tracks in the MetUM ensemble member and the reanalysis, or a weaker anticyclonic outflow as a result of the lack of explicit convection in ERA5.

The residuals are typically an order of magnitude smaller in the ERA5 data than in the MetUM simulations. The reason for this difference is not clear. One possibility is that the theory is less applicable to the MetUM simulations as the model is nonhydrostatic. Another possibility is that the convective noise on the borders of the domain is larger in the MetUM than in ERA5 as the former does not parameterize convection. The differences between the model time step and output time step probably do not explain the difference in magnitude of residuals. The IFS uses a time step of 12 min, the MetUM 75 s, and so, although the time output is far less frequent in ERA5, the ratio between the model time step and output time step in ERA5 ($60:12 \text{ min} = 5$) is comparable to that of the MetUM ($300:75 \text{ s} = 4$).

For the four regions at 01 UTC on 5 July 2016, the circulation tendency $\partial\Gamma/\partial t$ is calculated at the output time resolution of 5 min. The estimated circulation tendency (shown as the gray line in Figure 5) does not match the

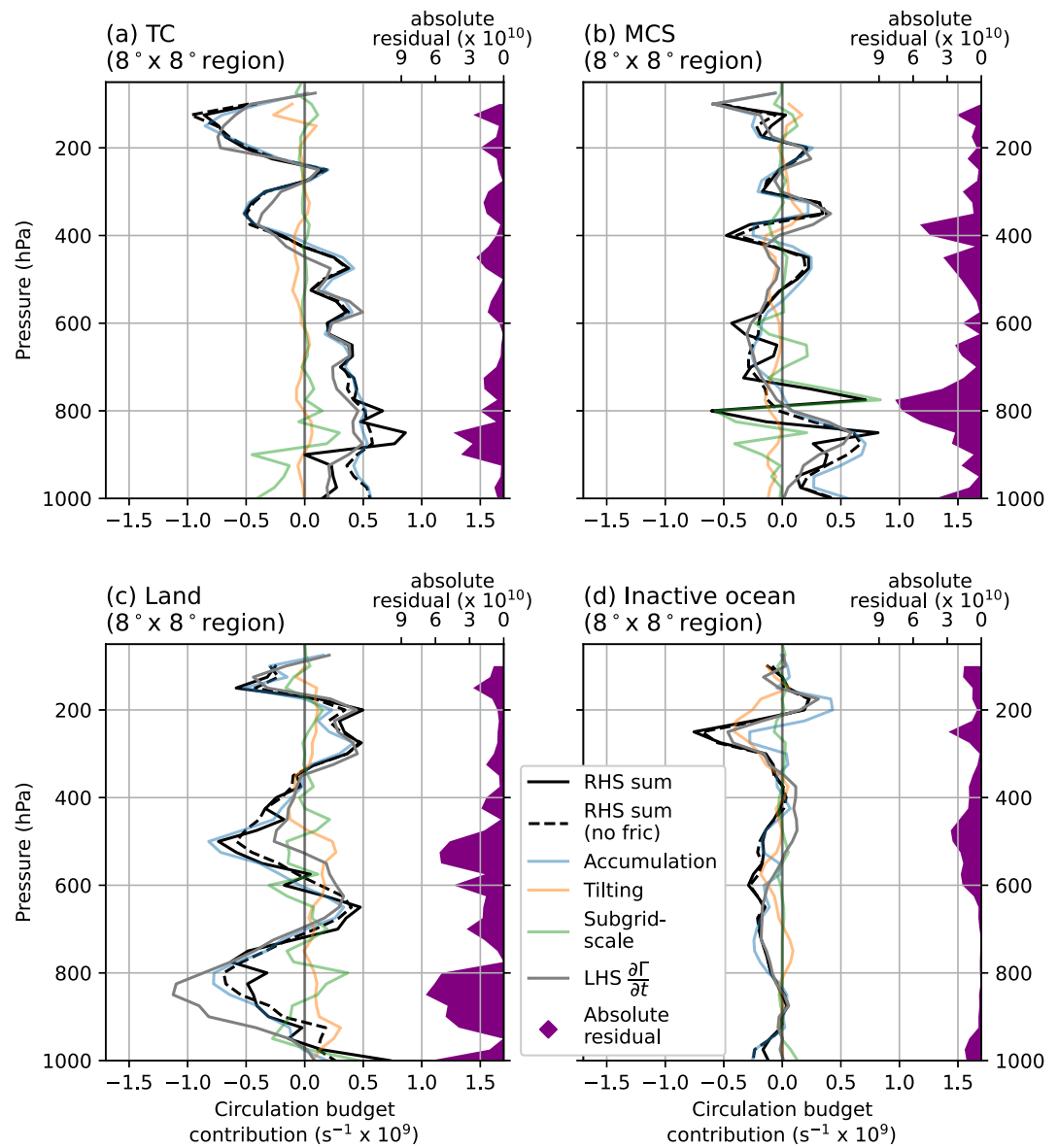


Figure 5. The circulation budget terms calculated around the $8 \times 8^\circ$ black boxes labeled (a–d) in Figure 2, at 01 UTC on 5 July 2016 in the simulation. The faded colored lines indicate the circulation budget terms calculated at each pressure level: the vorticity accumulation term (blue), the tilting term (orange), and the friction term (green). The black line is the sum of the three RHS terms. The gray line is the circulation tendency $\frac{\partial \Gamma}{\partial t}$ at the same time around the box, calculated at time output interval $\Delta t = 5$ min. The absolute residual at each pressure level is indicated by the filled purple region on the right-hand side of each axis (not on the same scale as the rest of the circulation budget contributions).

RHS sum of circulation budget terms exactly, although it captures many of the features of the vertical profile, largely matching the sign and following fluctuations in amplitude.

4.1. Sensitivity to the Inclusion of Subgrid-Scale Frictional Forces and the Domain

Where the convection straddles the border of the domain, errors are larger in the circulation tendency term and separate budget terms, leading to a poorer closure. Convection is a highly nonhydrostatic process, and so, the assumption of hydrostatic equilibrium does not hold. Violating this assumption introduces errors as discussed in Section 2, particularly in a convection-permitting model where the instantaneous values of the wind field near convection are likely to be noisy. The supplementary animation Movie S1 illustrates the circulation budget terms for the TC and land regions over the course of the simulation, and the associated column-integrated error at each

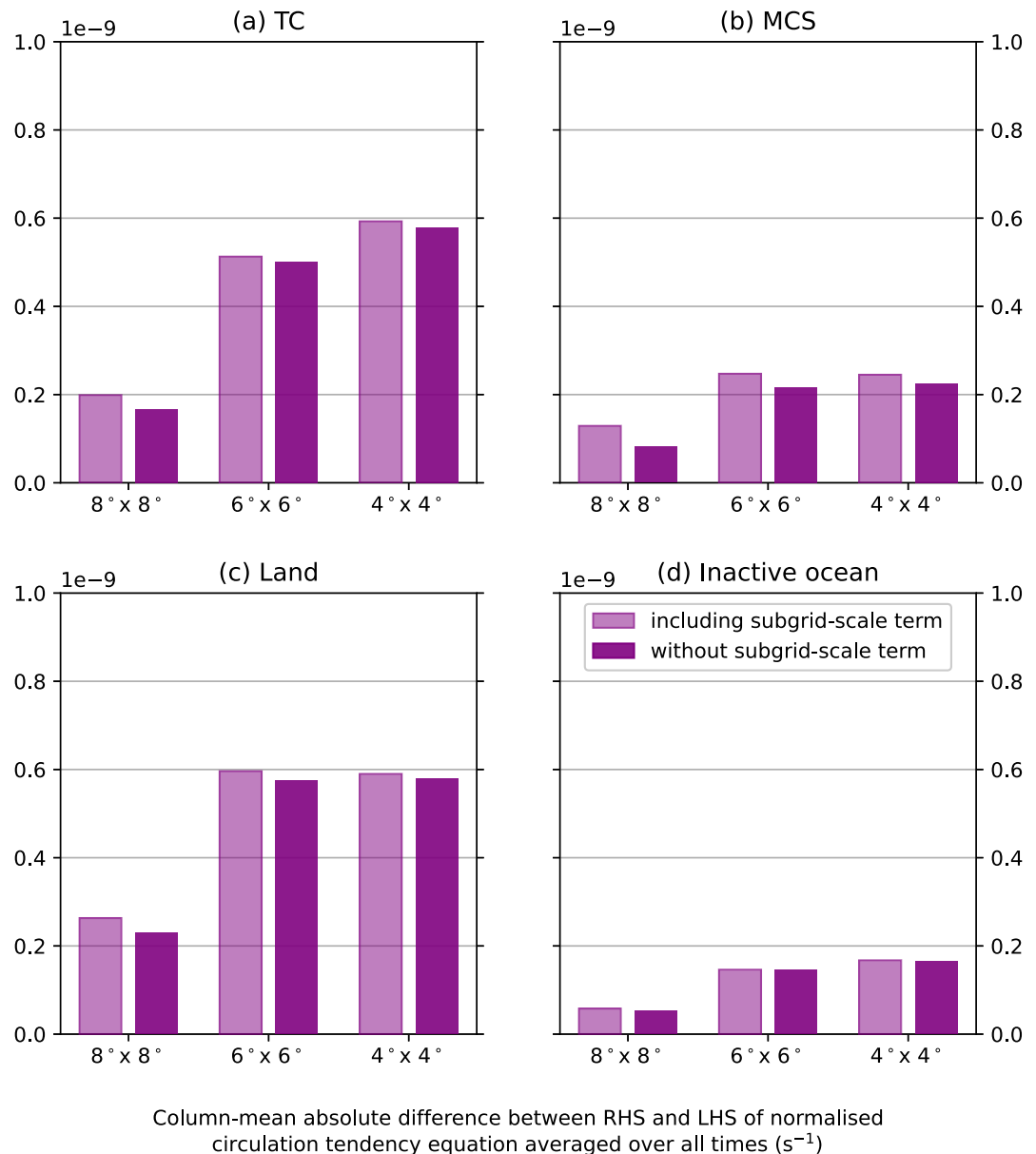


Figure 6. Normalized column-integrated mean absolute difference between sides of the circulation budget equation (Equation 4) for closure with (lighter shade) and without (darker shade) friction, for each of the four domains (a–d) illustrated in Figure 2 at different region sizes.

time. Animation Movie S1 indicates that, where convection crosses the border, the closure deteriorates; for example, as TC Nepartak enters the largest box of region A at 07 UTC on 4 July 2016, the NCIMAD almost triples from its value 6 hr before.

Estimates of the subgrid-scale term are made from Equation 5 with the stress tensor from the MetUM. Figure 5 shows that the subgrid-scale friction term (green line) is noisy, often introducing spikes in the RHS total profile (black line) and does not achieve better closure. Although friction is expected to be largest in the boundary layer where there is most turbulence, in these simulations, it varies noticeably throughout the profile, and is particularly noisy over land.

Figure 6 further illustrates the systematic differences in errors associated with the different regions. By far the highest values of NCIMAD are associated with domains over land or around the TC. These are the regions we would expect to deviate most strongly from hydrostatic balance; both regions appear convectively active (see

supplementary animation Movie S1), and the land region further contends with the effect of orography and surface fluxes associated with the terrestrial boundary layer.

Another element that may affect the circulation budget closure is the size of the domain. In addition to the $8 \times 8^\circ$ regions (black squares in Figure 2), the circulation budget is calculated on smaller $6 \times 6^\circ$ (blue) and $4 \times 4^\circ$ (cyan) regions centered on the same features. To evaluate the error associated with each domain size, the NCIMAD is calculated for the different-sized regions over the simulated period and plotted in Figure 6.

There is a distinct increase in the NCIMAD as the size of the domain decreases. An increase in error as domain size decreases is intuitive because, over the larger domains, the small-scale noise will be averaged out and will not be as strongly reflected in the mean differences. However, we hypothesize that the differences in the error between the domains are mostly to do with the variation in the wind field along the edges of the regions as explained above.

Figure 6 also indicates that including friction on the RHS of the equation results in a slightly increased error—unlike the ERA5 case, where including the subgrid-scale term in the budget improves closure noticeably. However, it should be noted that the MetUM output used is solely to calculate the effects of turbulent wind stress and is unlikely to be an accurate representation of all subgrid-scale processes. Without a subgrid-scale wind tendency term as we have in the ERA5 output, it is better to neglect the inaccurate version of subgrid-scale effects that is calculated here. Henceforth, the RHS of the circulation budget equation is calculated ignoring the friction term.

5. Effect of Temporal and Spatial Resolution

The circulation budget requires an estimate of the time derivative of circulation. If the wind fields are given at a time interval Δt , we expect that as Δt decreases, the truncation error in the derivative calculation will decrease. Note that Δt is not the time step of the numerical integration scheme used by the model, but rather the time interval at which the wind fields are stored. The calculation of $\partial\Gamma/\partial t$ uses central finite differencing with Δt as the time interval. Errors in the calculation of $\partial\Gamma/\partial t$ will therefore emerge from using a different differentiation method to the internal model solver, and from using a larger time step than the model calculation time step (75 s). We investigate now how the budget closure depends on Δt , which is chosen to be 5 min, 10 min, 20 min, 30 min, 1 hr, 3 hr, and 6 hr. The circulation tendencies are calculated for each of these values of Δt . In contrast, the RHS circulation budget terms are only calculated at 6-hourly intervals, as these calculations involve derivatives of the wind field at a single time and are unaffected by the choice of Δt .

Vertical profiles of circulation tendency calculated using different Δt are compared to the sum of the circulation budget terms calculated at a particular time and are shown in Figure 7. For $\Delta t \leq 30$ min, the vertical structure of $\partial\Gamma/\partial t$ appears to follow the same pattern as the $\Delta t = 5$ min case, albeit with increasingly weak amplitude. However, from about $\Delta t \geq 1$ hr, the patterns are substantially different, often with entire minima and maxima of the vertical profiles are missed; for example, in Figure 7c the maximum at around 650 hPa is missing in all the profiles with $\Delta t \geq 1$ hr.

The NCIMAD for the whole model run and the closure for the various choices of Δt in the four $8 \times 8^\circ$ regions are calculated and plotted in Figure 8. For all cases except region C (Figure 8), the increase in the error is negligible before $\Delta t = 1$ hr, and for all cases, the NCIMAD increases more rapidly between $\Delta t = 1$ hr and $\Delta t = 6$ hr. Figure 8 also supports the hypothesis that the closure is weaker when convection lies on the borders of a region. The highest errors occur over land, where there is regularly active convection, and in the TC region, where Nepartak transitions through the boundaries in and out of the box during the time period.

The tendency of the highest time resolutions to most closely match the instantaneous RHS sum of circulation terms implies that the RHS terms are an exact measure of the circulation tendency (other than the subgrid-scale processes that are not calculated explicitly here). When the ERA5 subgrid-scale terms are included, the closure is very good, even at low time resolutions, which implies that the calculations of the tilting and accumulation terms are accurate. Therefore, even if it is not possible to calculate all terms in the circulation budget, or if the closure is limited by the frequency of the output data, the RHS circulation budget terms are accurate enough to meaningfully quantify the processes involved in modulating circulation.

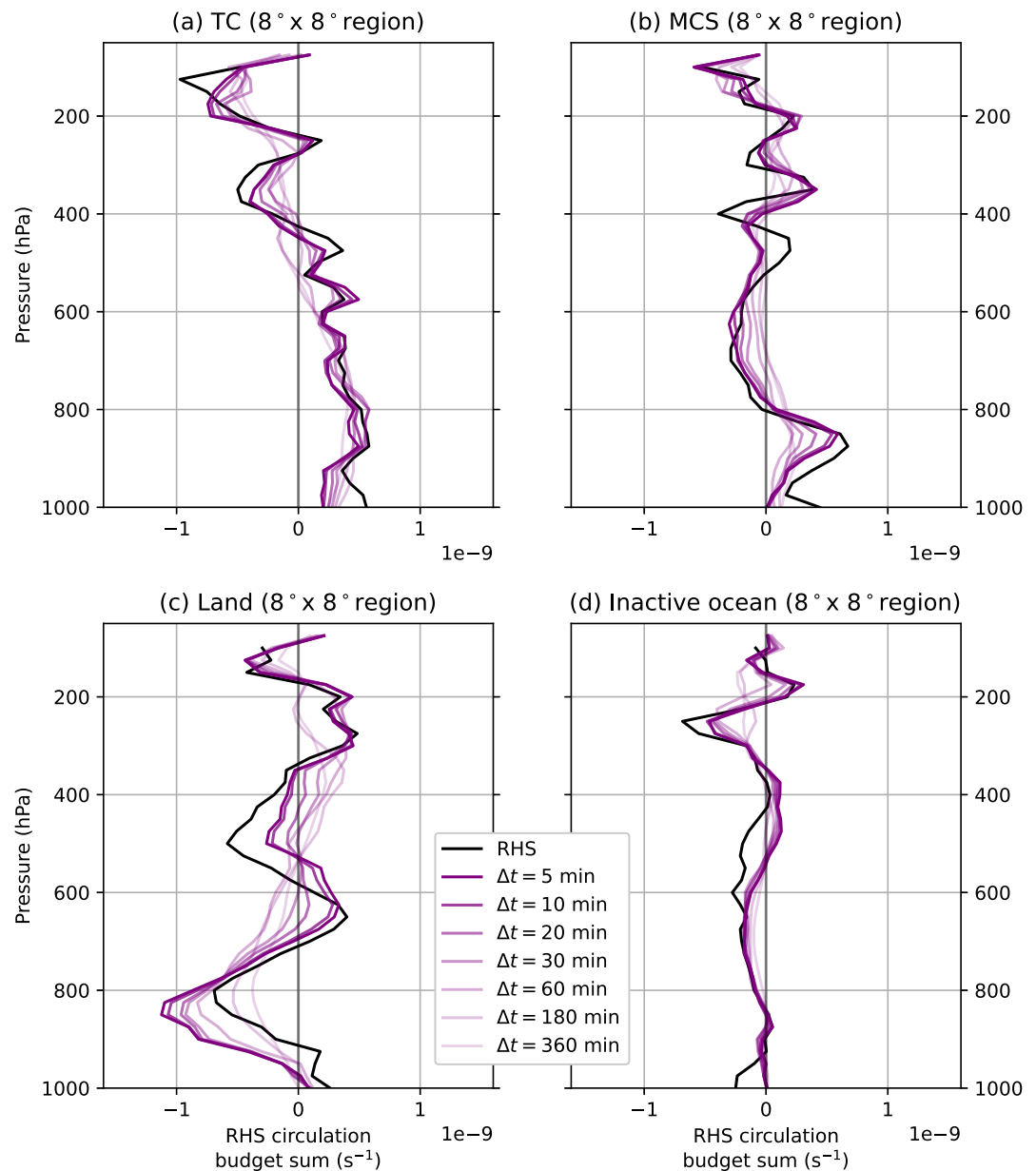


Figure 7. Circulation tendency for various Δt calculated around the $8 \times 8^\circ$ black boxes labeled (a–d) in Figure 2, at 01 UTC on 5 July in the simulation. The dashed black line indicates the RHS sum of circulation budget terms whereas the purple lines represent different Δt as illustrated in the legend.

Another aspect of model configuration that may affect the circulation budget is the spatial resolution, since output data with high spatial resolution are not always available. To replicate output from coarser model grids, the model output is regridded to have horizontal grid lengths of Δx of 0.1° , 0.15° , 0.2° , and 0.25° . The instantaneous circulation budget terms and circulation tendency terms are calculated for each grid spacing. The regridding uses a linear regridding algorithm provided by xarray (Hoyer et al., 2022; Hoyer & Hamman, 2017). The RHS of the circulation budget equations (the sum of the instantaneous circulation budget terms) for the sample time of 01 UTC on 5 July 2016 (captured by Figure 2) is shown in Figure 9.

Figure 9 indicates that changing grid spacing can significantly change the sum of instantaneous RHS circulation budget terms; for regions A–C (Figures 9a–9c), the profiles at 0.2° resolution differ in both magnitude and sign from corresponding profiles at 0.04° resolution. Coarsening spatial resolution affects both the LHS and RHS of

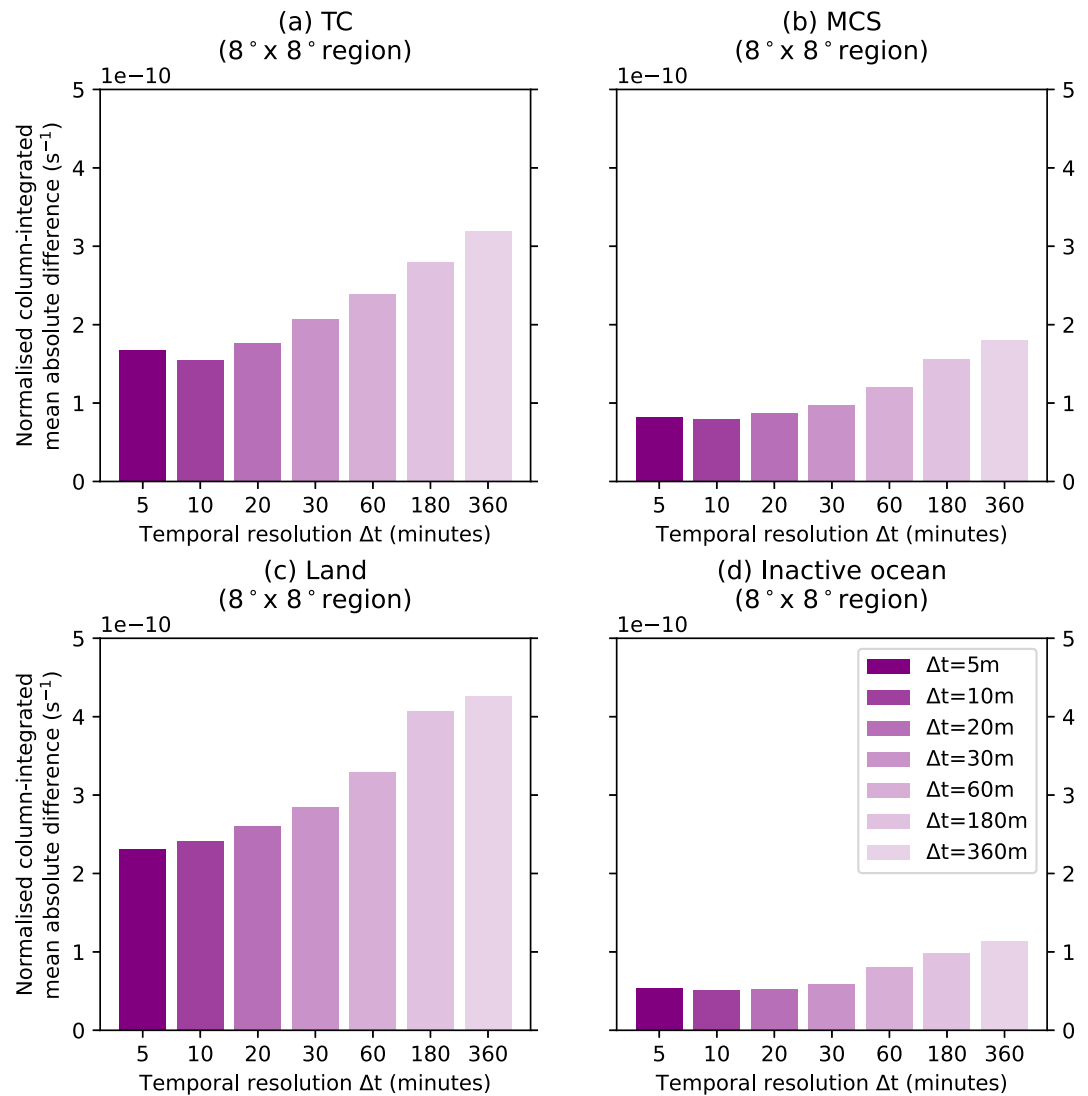


Figure 8. Normalized column-integrated mean absolute difference between both sides of the circulation budget equation for different Δt . Circulation budget terms and the circulation are calculated around the regions (a–d) shown in Figure 2.

the circulation budget. If the process affects both sides of the equation in the same way, then closure may not necessarily worsen. To explore whether closure generally worsens with coarsening spatial resolution, we present the mean NCIMAD for the $8 \times 8^\circ$ boxes over the simulation period in Figure 10. For each spatial resolution, a corresponding circulation tendency is evaluated using $\Delta t = 5$ minutes, and there is a consistent trend in worsening closure with coarser spatial resolution.

Having evaluated the effect of varying both the spatial and temporal resolution independently, the next step is to covary both output resolutions. Figure 11 shows the NCIMAD over the model run. As may be anticipated, the best closure for each region has the highest spatial and temporal resolution. The closure worsens more dramatically with the coarsening of the spatial resolution than the coarsening of temporal output. Moreover, as in the previous examples, the largest errors in closure lie in the TC and land regions.

NCIMAD increases as temporal and spatial resolutions decrease, except when $\Delta x = 0.25^\circ$, where the ratio has a minimum at a temporal resolution of around $\Delta t = 30$ minutes for most of the regions. Perhaps as the spatial and temporal resolutions decrease, they both reduce variation in the vertical profile in the same way, and thus, the LHS and RHS profiles are more similar. Therefore, while there may be a better closure with larger output time steps

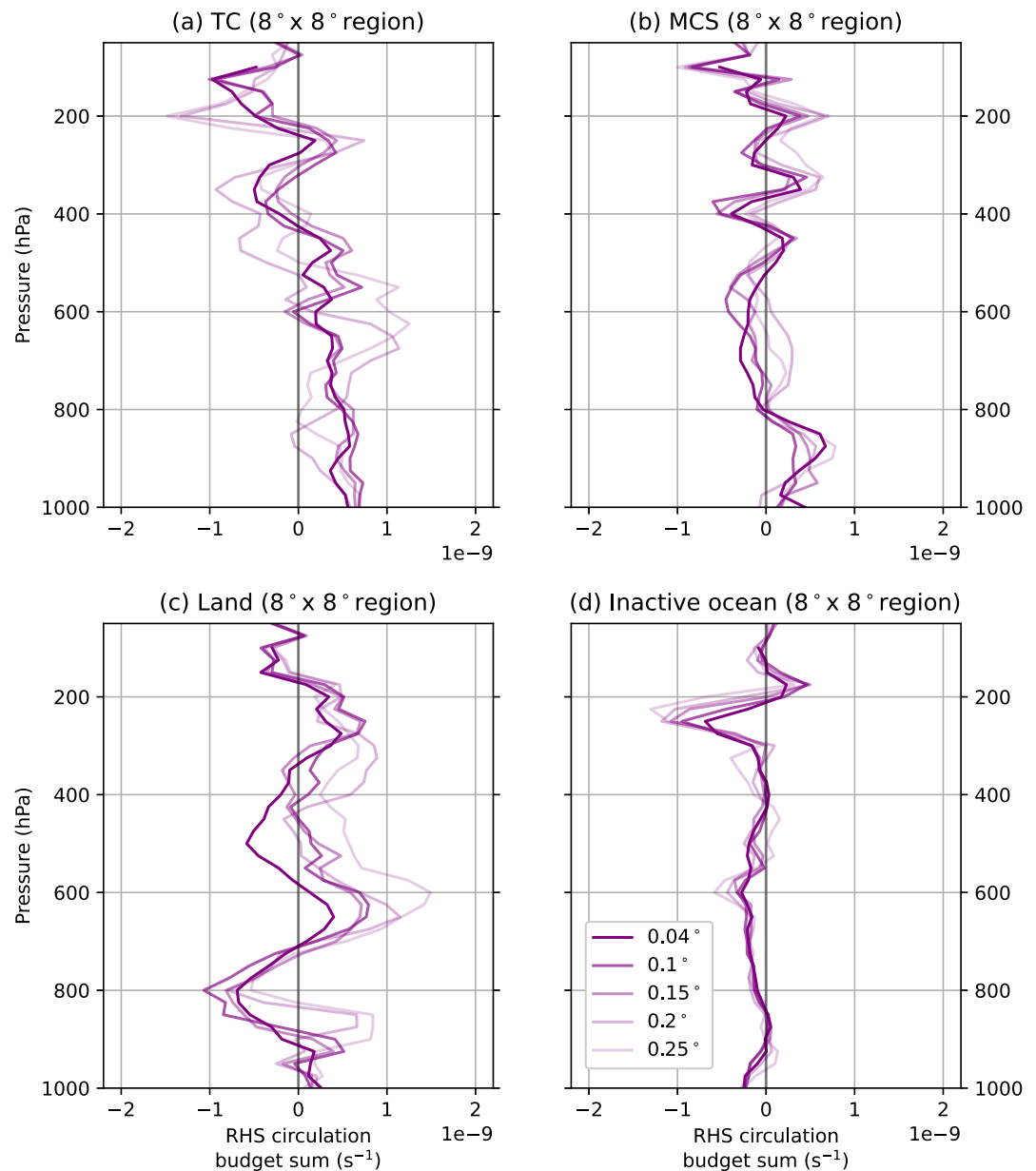


Figure 9. RHS of circulation budget profiles calculated for different spatial resolutions Δx , shown for 01 UTC on 05 July 2016 and regions (a–d) outlined in Figure 2. The native grid resolution is the highest resolution shown, 0.04° .

with low-resolution output, the values of both sides of the equation may be further from the absolute truth and the circulation budget terms may provide less meaningful insight into the processes affecting circulation.

6. Conclusions

This study outlines a methodology for calculating the circulation budget. It also evaluates how the closure of the circulation budget is affected by the omission of subgrid-scale momentum transport, and the effect of the truncation errors associated with numerical differentiation in time and space. The latter factor is relevant because, in practice, coarser spatiotemporal resolutions are often used in analysis due to limitations on the storage of large data sets from model runs or reanalyses.

The first aim of the study is to assess how well the circulation budget closes without knowing F . Many studies that use the circulation budget either comment that the subgrid-scale contributions can be estimated using the budget

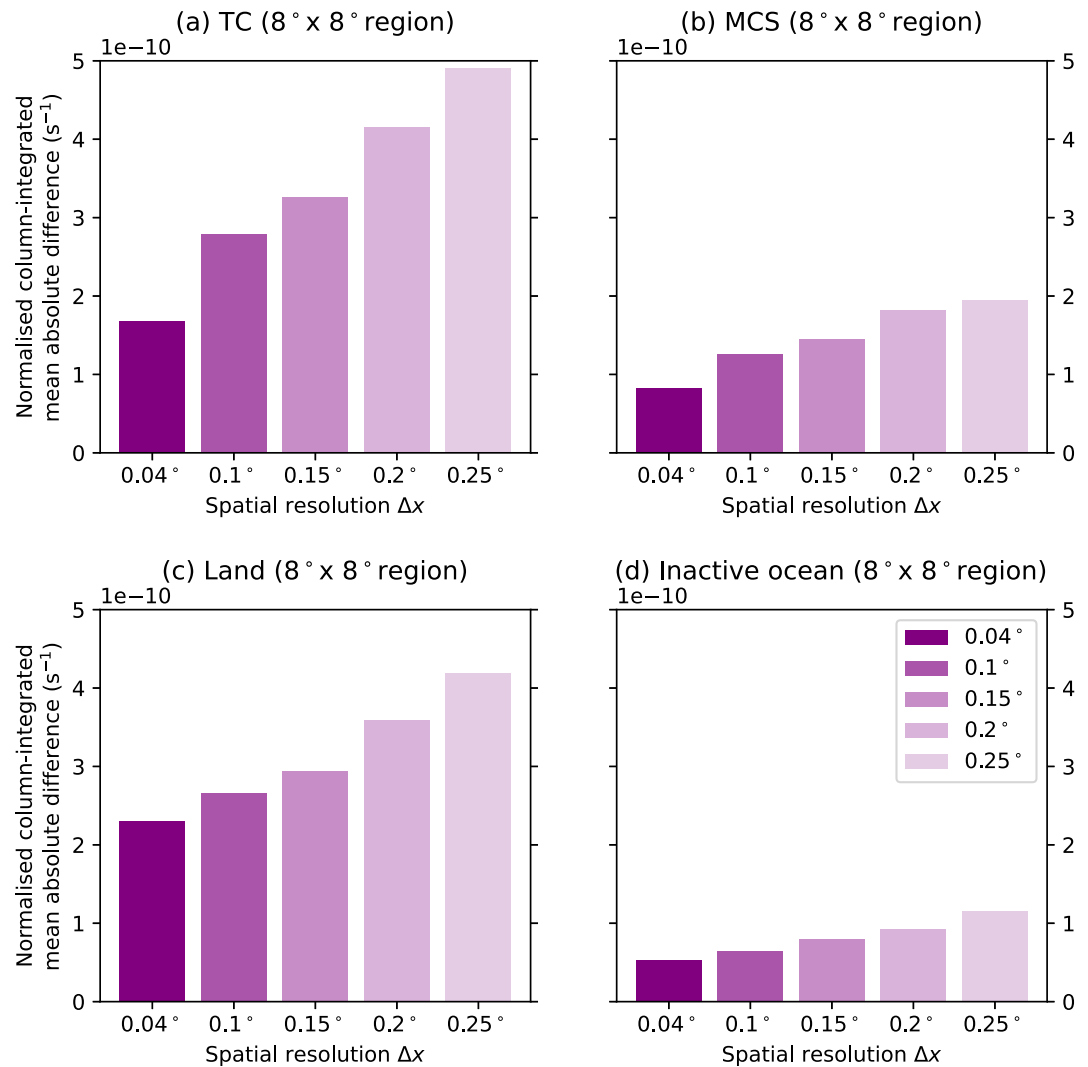


Figure 10. Normalized column-integrated mean absolute difference for different Δx over the simulation period. Circulation budget terms and circulation are calculated around the regions (a–d) shown in Figure 2, at the respective grid resolutions Δx corresponding to each bar. The native grid resolution is the highest resolution shown, 0.04° .

residual, or they replace the term with an exponential vertical profile adjusted to a scale height associated with the boundary layer, which approximates the atmospheric friction over the ocean. Here, we explicitly calculate the subgrid-scale contributions to the circulation budget using stress tensor model output in the MetUM and general subgrid-scale wind tendencies in ERA5. For ERA5, including subgrid-scale tendencies significantly improves the budget closure, especially over land and in regions where there is turbulent motion on the edges of the domain. However, the MetUM turbulent stress tensor output is noisy, which leads to a poorer closure than excluding the term entirely. While there may be uncertainties associated with the parameterizations used in the ERA5 representation of the subgrid term, these are much smaller than other formulations for the subgrid term, including the aforementioned estimates from wind stress terms or assumed exponential vertical profiles. Other errors may arise in the circulation budget calculation: for example, the data assimilation cycle pushes the ERA5 budget further from closure, the selection of domain can introduce errors (see next paragraph), and errors are introduced by truncation effects in numerical differentiation and integration. While smoothing with a moving average can reduce the residuals, it may remove convective signals which are of interest at higher temporal resolutions. In practice, the amount of smoothing may depend on the user's interests; for example, a study of the diurnal cycle of convection should likely use shorter (or even no) averaging periods. For model studies, the lack of data assimilation may also mean less smoothing is required.

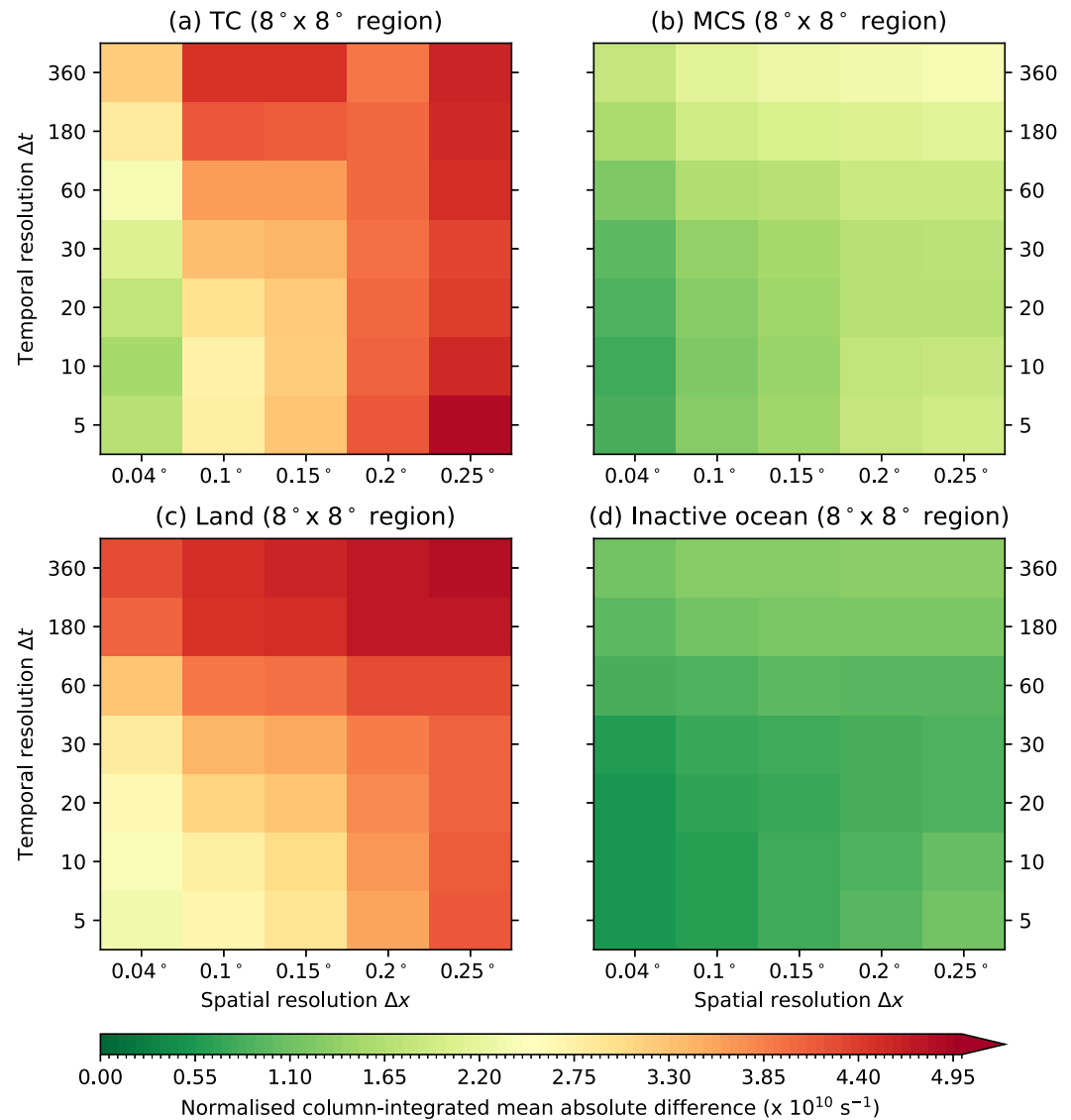


Figure 11. Normalized column-integrated mean absolute difference for different Δx (horizontal axis) and Δt (vertical axis), calculated over the whole model run for the regions (a–d) shown in Figure 2.

The second aim of the study is to evaluate the sensitivity of the circulation budget to the choice of the domain. When selecting a region in which to calculate the circulation budget, it is best to avoid sharply fluctuating wind field on the domain edges. Ideally, the region should fully enclose the convection. Nonhydrostatic atmospheric profiles mean that the budget closure is violated, because it is derived assuming a hydrostatic atmosphere. Where subgrid-scale terms are not calculated, errors in the budget closure increase more dramatically in regions with convection on boundaries; for example, see the significantly larger NCIMAD in the TC and land regions in the MetUM simulations than the inactive ocean region (Figure 6). These errors are further amplified as fewer grid points are sampled (i.e., with coarsening spatial resolution; see Figure 10). While convection on the domain boundaries may limit the accuracy of the budget closure, it may still be of interest and can contribute to the circulation tendency through the tilting and subgrid-scale terms. Therefore, regardless of closure, this method can be an effective way of evaluating convection-circulation interactions from a process-based perspective.

The third aim of the study is to evaluate how closure of the circulation budget changes with spatial and temporal resolution of the output. The calculation of circulation budget terms and tendency relies on numerical differentiation and integration. The two models in this study (IFS and MetUM) use an internal SISL solver to calculate

derivatives and integrate over time steps, whereas the typical analysis of standard model output will use simpler techniques such as first- or second-order centered finite differencing; the difference between these methods will introduce errors. Furthermore, the derivatives are calculated using model output time steps (which are typically on the order of hours) which are larger than model calculation time steps (on the order of seconds to minutes). The degree of closure systematically worsens as the output time interval increases. For a user running a model simulation where outputs will be used to compute a circulation budget, results in this paper imply that if coarsening of temporal resolution is required, it should be limited to output intervals of 30 min (approximately 25 times the model calculation time step) in order to capture the vertical profile of circulation tendency accurately.

Coarsening spatial resolution also systematically increases the error in budget closure. Furthermore, altering the spatial sampling can significantly change the circulation budget, and so, inferences about the circulation budget from regridded data should be made with caution. Despite the relatively coarse grid spacing, the circulation budget from ERA5 closes well even without the inclusion of the subgrid-scale term. One reason for this is that its output is on its native grid, so no errors are introduced through spatial resampling. A second reason is that the IFS is hydrostatic, as is the circulation budget formulation, but the MetUM is nonhydrostatic. If spatial resampling is necessary, the results in this paper imply that it is best to resample to no coarser than 3 times the native model grid spacing (in this case, 0.15°) in order to retain characteristics of the vertical profile of the circulation budget (roughly equivalent to the temporal coarsening to output intervals of 30 min).

The ultimate goal of the study is to establish whether the conclusions drawn from a circulation budget calculation that did not close could be meaningful. Even when the time derivative (LHS) cannot be accurately calculated because the data have insufficient time resolution, the circulation budget terms (RHS) remain accurate so long as the fields are instantaneous values. Therefore, the circulation budget terms are still physically meaningful at their instantaneous output time, regardless of the model output time step. However, where models are resampled to lower spatial resolutions, particularly at 0.15° or coarser, and particularly in regions where there is active convection, the validity of inferences drawn from the circulation budget are less certain. Regardless, on a native model output grid, the circulation budget terms calculated from instantaneous fields will be accurate and are an extremely useful tool for process-oriented analysis in meteorology and climate science.

Data Availability Statement

Reanalysis data are from ERA5 (Hersbach et al., 2020). MetUM data are not publicly available but can be obtained on request subject to Met Office licensing. Software used to calculate circulation budgets is available in a Zenodo repository (Morris & Robinson, 2024).

References

- Bush, M., Allen, T., Bain, C., Boutle, I., Edwards, J., Finnenkoetter, A., et al. (2020). The first met office unified model–JULES regional atmosphere and land configuration, RAL1. *Geoscientific Model Development*, 13(4), 1999–2029. <https://doi.org/10.5194/gmd-13-1999-2020>
- Chen, T.-C., Yau, M.-K., & Kirshbaum, D. J. (2020). Towards the closure of momentum budget analyses in the WRF (v3.8.1) model. *Geoscientific Model Development*, 13(3), 1737–1761. <https://doi.org/10.5194/gmd-13-1737-2020>
- Cram, T. A., Montgomery, M. T., & Hertenstein, R. F. A. (2002). Early evolution of vertical vorticity in a numerically simulated idealized convective line. *Journal of the Atmospheric Sciences*, 59(13), 2113–2127. [https://doi.org/10.1175/1520-0469\(2002\)059<2113:EEOVVI>2.0.CO;2](https://doi.org/10.1175/1520-0469(2002)059<2113:EEOVVI>2.0.CO;2)
- Davis, C. A., & Galareau, T. J. (2009). The vertical structure of mesoscale convective vortices. *Journal of the Atmospheric Sciences*, 66(3), 686–704. <https://doi.org/10.1175/2008JAS2819.1>
- Duran, P., & Molinari, J. (2019). Tropopause evolution in a rapidly intensifying tropical cyclone: A static stability budget analysis in an idealized axisymmetric framework. *Journal of the Atmospheric Sciences*, 76(1), 209–229. <https://doi.org/10.1175/JAS-D-18-0097.1>
- Fu, S.-M., Li, W.-L., & Ling, J. (2015). On the evolution of a long-lived mesoscale vortex over the Yangtze River Basin: Geometric features and interactions among systems of different scales. *Journal of Geophysical Research: Atmospheres*, 120(23). <https://doi.org/10.1002/2015JD023700>
- Hardy, S., Schwendike, J., Smith, R. K., Short, C. J., Reeder, M. J., & Birch, C. E. (2021). Fluctuations in inner-core structure during the rapid intensification of super typhoon nepartak (2016). *Monthly Weather Review*, 149(1), 221–243. <https://doi.org/10.1175/MWR-D-19-0415.1>
- Haynes, P. H., & McIntyre, M. E. (1987). On the evolution of vorticity and potential vorticity in the presence of diabatic heating and frictional or other forces. *Journal of the Atmospheric Sciences*, 44(5), 828–841. [https://doi.org/10.1175/1520-0469\(1987\)044<0828:OTEOVA>2.0.CO;2](https://doi.org/10.1175/1520-0469(1987)044<0828:OTEOVA>2.0.CO;2)
- Hersbach, H., Bell, B., Berrisford, P., Hirahara, S., Horányi, A., Muñoz-Sabater, J., et al. (2020). The ERA5 global reanalysis. *Quarterly Journal of the Royal Meteorological Society*, 146(730), 1999–2049. <https://doi.org/10.1002/qj.3803>
- Hodur, R. M., & Fein, J. S. (1977). A vorticity budget over the Marshall Islands during the spring and summer months. *Monthly Weather Review*, 105(12), 1521–1526. [https://doi.org/10.1175/1520-0493\(1977\)105<1521:AVBOTM>2.0.CO;2](https://doi.org/10.1175/1520-0493(1977)105<1521:AVBOTM>2.0.CO;2)
- Hoyer, S., & Hamman, J. (2017). Xarray: N-D labeled arrays and datasets in Python. *Journal of Open Research Software*, 5(1), 10. <https://doi.org/10.5334/jors.148>
- Hoyer, S., Roos, M., Joseph, H., Magin, J., Cherian, D., Fitzgerald, C., et al. (2022). Xarray. *Zenodo*. <https://doi.org/10.5281/ZENODO.7293617>

Acknowledgments

We are grateful to Christian Jakob and Sugata Narsey for their insightful comments on this work. This study was supported by the following funding sources.

- Leeds-York-Hull Natural Environment Research Council Doctoral Training Partnership Panorama, Grant NE/S007458/1 (FM PhD studentship)
- Australian Government Research Training Program Scholarship (CR PhD studentship)
- Australian Research Council Center of Excellence for Climate extremes, fund number CE170100023 (supporting CR and MR)
- Met Office Newton Fund Weather for Climate Services (WCSSP) Southeast Asia (supporting JS and the generation of MetUM simulations utilized in the paper).
- First Rains: UKRI Future Leaders Fellowship MR/W011379/1 (supporting FM as a postdoctoral researcher on the project).

- Kanamitsu, M., & Saha, S. (1996). Systematic tendency error in budget calculations. *Monthly Weather Review*, *124*(6), 1145–1160. [https://doi.org/10.1175/1520-0493\(1996\)124<1145:STEIBC>2.0.CO;2](https://doi.org/10.1175/1520-0493(1996)124<1145:STEIBC>2.0.CO;2)
- Kiranmayi, L., & Maloney, E. D. (2011). Intraseasonal moist static energy budget in reanalysis data: Intraseasonal MSE budget in NCEP and ERA. *Journal of Geophysical Research*, *116*(D21). <https://doi.org/10.1029/2011JD016031>
- Kutty, G., & Gohil, K. (2017). The role of mid-level vortex in the intensification and weakening of tropical cyclones. *Journal of Earth System Science*, *126*(7), 94. <https://doi.org/10.1007/s12040-017-0879-y>
- Matthews, A. J. (2021). Dynamical propagation and growth mechanisms for convectively coupled equatorial Kelvin waves over the Indian Ocean. *Quarterly Journal of the Royal Meteorological Society*, *147*(741), 4310–4336. <https://doi.org/10.1002/qj.4179>
- Morris, F., & Robinson, C. M. (2024). Closing the Circulation Budget - Code to calculate and create figures [Software]. <https://doi.org/10.5281/zenodo.14218296>
- Morris, F., Schwendike, J., Parker, D. J., & Bain, C. (2024). How is synoptic-scale circulation influenced by the dynamics of mesoscale convection in convection-permitting simulations over west Africa? *Journal of the Atmospheric Sciences*, *81*(4), 765–782. <https://doi.org/10.1175/JAS-D-22-0032.1>
- Neelin, J. D., & Held, I. M. (1987). Modeling tropical convergence based on the moist static energy budget. *Monthly Weather Review*, *115*(1), 3–12. [https://doi.org/10.1175/1520-0493\(1987\)115<0003:MTCBOT>2.0.CO;2](https://doi.org/10.1175/1520-0493(1987)115<0003:MTCBOT>2.0.CO;2)
- Noda, A. T., & Niino, H. (2010). A numerical investigation of a supercell Tornado: Genesis and vorticity budget. *Journal of the Meteorological Society of Japan. Ser. II*, *88*(2), 135–159. <https://doi.org/10.2151/jmsj.2010-203>
- Penny, A. B., Harr, P. A., & Doyle, J. D. (2016). Sensitivity to the representation of microphysical processes in numerical simulations during tropical storm formation. *Monthly Weather Review*, *144*(10), 3611–3630. <https://doi.org/10.1175/MWR-D-15-0259.1>
- Raymond, D., Gjorgjievska, S., Sessions, S., & Fuchs, K. (2014). Tropical cyclogenesis and mid-level vorticity. *Australian Meteorological and Oceanographic Journal*, *64*(1), 11–25. <https://doi.org/10.22499/2.6401.003>
- Raymond, D. J., & Carrillo, C. L. (2011). The vorticity budget of developing typhoon Nuri (2008). *Atmospheric Chemistry and Physics*, *11*(1), 147–163. <https://doi.org/10.5194/acp-11-147-2011>
- Roberts, B., Xue, M., & Dawson, D. T. (2020). The effect of surface drag strength on mesocyclone intensification and tornadogenesis in idealized supercell simulations. *Journal of the Atmospheric Sciences*, *77*(5), 1699–1721. <https://doi.org/10.1175/JAS-D-19-0109.1>
- Sanders, F., & Emanuel, K. A. (1977). The momentum budget and temporal evolution of a mesoscale convective system. *Journal of the Atmospheric Sciences*, *34*(2), 322–330. [https://doi.org/10.1175/1520-0469\(1977\)034<0322:TMBATE>2.0.CO;2](https://doi.org/10.1175/1520-0469(1977)034<0322:TMBATE>2.0.CO;2)
- Schwendike, J., & Jones, S. C. (2010). Convection in an African easterly wave over west Africa and the eastern Atlantic: A model case study of Helene (2006). *Quarterly Journal of the Royal Meteorological Society*, *136*(S1), 364–396. <https://doi.org/10.1002/qj.566>
- Shapiro, L. J. (1978). The vorticity budget of a composite African tropical wave disturbance. *Monthly Weather Review*, *106*(6), 806–817. [https://doi.org/10.1175/1520-0493\(1978\)106<0806:TVBOAC>2.0.CO;2](https://doi.org/10.1175/1520-0493(1978)106<0806:TVBOAC>2.0.CO;2)
- Shu, Y., Sun, J., Jin, C., & Zhuang, B. (2022). Vorticity budget and formation mechanisms of a mesoscale convective vortex in a heavy-rainstorm episode. *Atmosphere*, *13*(4), 556. <https://doi.org/10.3390/atmos13040556>
- Stevens, D. E. (1979). Vorticity, momentum and divergence budgets of synoptic-scale wave disturbances in the tropical eastern Atlantic. *Monthly Weather Review*, *107*(5), 535–550. [https://doi.org/10.1175/1520-0493\(1979\)107<0535:VMADBO>2.0.CO;2](https://doi.org/10.1175/1520-0493(1979)107<0535:VMADBO>2.0.CO;2)
- Van Der Wiel, K., Matthews, A. J., Stevens, D. P., & Joshi, M. M. (2015). A dynamical framework for the origin of the diagonal South Pacific and South Atlantic convergence zones. *Quarterly Journal of the Royal Meteorological Society*, *141*(691), 1997–2010. <https://doi.org/10.1002/qj.2508>
- Wang, Z. (2012). Thermodynamic aspects of tropical cyclone formation. *Journal of the Atmospheric Sciences*, *69*(8), 2433–2451. <https://doi.org/10.1175/JAS-D-11-0298.1>
- Wang, Z., Montgomery, M. T., & Dunkerton, T. J. (2010). Genesis of pre-hurricane Felix (2007). Part I: The role of the easterly wave critical layer. *Journal of the Atmospheric Sciences*, *67*(6), 1711–1729. <https://doi.org/10.1175/2009JAS3420.1>
- Wood, N., Staniforth, A., White, A., Allen, T., Diamantakis, M., Gross, M., et al. (2014). An inherently mass-conserving semi-implicit semi-Lagrangian discretization of the deep-atmosphere global non-hydrostatic equations. *Quarterly Journal of the Royal Meteorological Society*, *140*(682), 1505–1520. <https://doi.org/10.1002/qj.2235>